Open Access Full Text Article

ORIGINAL RESEARCH

Bergamottin Induces DNA Damage and Inhibits Malignant Progression in Melanoma by Modulating miR-145/Cyclin D1 Axis

Zhongfang Zhao
Nong Liao

Department of Plastic and Cosmetic Surgery, The Third Affiliated Hospital of Guangzhou Medical University, Guangzhou City, Guangdong Province, 510150, People's Republic of China

Background: Melanoma is a prevalent skin cancer with the high rate of metastasis and mortality, affecting the increasing number of people worldwide. Bergamottin (BGM) is a natural furanocoumarin derived from grapefruits and presents the potential anti-cancer activity in several tumor models. However, the role of BGM in the development of melanoma remains unclear. Here, we aimed to explore the effect of BGM on the DNA damage and progression of melanoma.

Methods: The effect of BGM on the melanoma progression was analyzed by CCK-8 assays, colony formation assays, transwell assays, Annexin V-FITC Apoptosis Detection Kit, cell-cycle analysis, in vivo tumorigenicity analysis. The mechanism investigation was performed using luciferase reporter gene assays, qPCR assays, and Western blot analysis.

Results: We identified that BGM repressed cell proliferation, migration, and invasion of melanoma cells. BGM induced cell cycle arrest at the G0/G1 phase and enhanced apoptosis of melanoma cells. The DNA damage in the melanoma cells was stimulated by the BGM treatment. Meanwhile, BGM was able to up-regulate the expression of miR-145 and miR-145 targeted Cyclin D1 in the melanoma cells. Furthermore, BGM inhibited the progression of melanoma by targeting miR-145/Cyclin D1 axis in vitro. BGM attenuated the tumor growth of melanoma in vivo.

Conclusion: Thus, we conclude that BGM induces DNA damage and inhibits tumor progression in melanoma by modulating the miR-145/Cyclin D1 axis. Our finding provides new insights into the mechanism by which BGM modulates the development of melanoma. BGM may be applied as a potential anti-tumor candidate for the clinical treatment of melanoma.

Keywords: melanoma, progression, DNA damage, bergamottin, miR-145, Cyclin D1

Introduction

Melanoma serves as a prevalent malignant cancer that is accountable for 80% of mortality of all skin cancer, with extraordinary metastasis and aggressive.[1,2] The occurrence of melanoma steadily continues growing around the world.[3] In the past decades, despite some advancements accomplished, patients with melanoma still exhibit poor prognosis due to resistance to radiotherapy or chemotherapy and metastasis.[4] Surgical/drug intervention, control metabolism, and early diagnosis were the valid therapy strategies for melanoma patients,[5–7] but the progression and underlying mechanism of melanoma at the molecular level remained mostly unknown, which is required to be further studied.[8] Moreover, DNA damage, as

Correspondence: Nong Liao
Department of Plastic Surgery, The Third Affiliated Hospital of Guangzhou Medical University, No. 63 Duobao Road, Liwan District, Guangzhou City, Guangdong Province, 510150, People's Republic of China
Email nongliaoduobao@163.com

a critical process and the therapeutic target of cancers, plays an essential role in the development of melanoma. More importantly, although advanced development has been made in melanoma therapies, such as immunotherapies and targeted therapies, response to these treatments is usually featured by heterogeneous and not durable.[9,10] Therefore, it is urgently needed to explore more practical therapeutic candidates for melanoma.

The demand for the novel and lower toxicity anti-cancer medicine development has directed to investigate the potentially useful anti-cancer compounds in herbs, vegetables, and fruits.[11,12] Grapefruit furanocoumarins have displayed several pharmacological impacts, such as bone health-promoting effects and anti-cancer activities.[13] Bergamottin (BGM) is a significant furanocoumarin derived from grapefruits (Citrus paradise) and has presented to be a potential anti-cancer candidate in several preclinical mouse models and cancer cell lines.[14] For example, the previous investigation demonstrated that BGM inhibits the growth of multiple myeloma cells and leads to programmed cell death by the modulation of the STAT3 pathway.[15] However, the effect of BGM on the development of melanoma remains unclear.

MicroRNAs (miRNAs) are small, stable single-stranded non-coding RNAs that present an essential function in post-transcriptional gene regulation through targeting mRNAs, repressing their translation, or causing its degradation.[16,17] MiRNAs possess pleiotropic influences due to interacting with various mRNAs by a microRNA, playing a notable role in the modulation of cancer development.[18,19] Thus, they can serve as biomarkers and targets for the treatment of cancers.[20] Recent studies reveal that miRNAs regulate not only crucial pathways leading to melanoma progression and development but also are able to influence the drug resistance of melanoma.[21–23] Meanwhile, it has been identified that miR-145 is aberrantly expressed in melanoma and is involved in the modulation of melanoma.[24,25] Besides, Cyclin D1, as a cell-cycle process regulator, is a crucial contributor to cancer progression.[26,27] MiR-145 has been reported to inhibit the expression of Cyclin D1.[28] However, the impact of BGM on miR-145 and the correlation of and miR-145 with Cyclin D1 in the development of melanoma remain unreported.

In this study, we aimed to explore the effect of BGM on melanoma development. We identified a novel function of BGM in inducing DNA damage and inhibiting melanoma progression by modulating miR-145/Cyclin D1 axis.

Methods
Cell Culture and Treatment
The human melanoma WM239 and MM200 cells were purchased in American Type Tissue Culture Collection. The cells were cultured in the medium of RPMI 1640 (Gibco, USA) containing 10% fetal bovine serum (Gibco, USA), 0.1 mg/mL streptomycin (Solarbio, China) and 100 units/mL penicillin (Solarbio, China) at a condition of 37°C with 5% CO_2. Bergamottin (BGM, purity >98%, monohydrate) was obtained from Biyang (Chengdu, China). The structural formula of BGM was shown in Figure S1. The cells were treated with BGM at the indicated dose for further analysis. The miR-145 mimic, control mimic, miR-145 inhibitor, control inhibitor, pcDNA 3.1 vector, and pcDNA 3.1-Cyclin D1 overexpression vector were obtained (GenScript, China) (GenePharma, China). The mice needed for the experiment were provided by the Third Affiliated Hospital of Guangzhou Medical University. The transfection in the cells was performed by Liposome 3000 (Invitrogen, USA) according to the manufacturer's instructions.

CCK-8 Assays
The cell viability was analyzed by the CCK-8 assays. About $5×10^3$ cells were put into 96 wells and cultured for 12 hours. Then the cells were used for the transfection or treatment. After 0 hours, 24 hours, 48 hours, 72 hours, and 96 hours, the cells were added with a CCK-8 solution (KeyGEN Biotech, China) and culture for another 2 hours at 37°C. The ELISA browser was applied to analyze the absorbance at 450nm (Bio-Tek EL 800, USA).

Colony Formation Assays
About $1×10^3$ cells were layered in 6 wells and incubated in RPMI 1640 at 37°C. After two weeks, cells were cleaned with PBS Buffer, made in methanol for about thirty minutes, and dyed with crystal violet dye at the dose of 1%, after which the number of colonies was calculated.

Transwell Assays
Transwell assays analyzed the impacts of MI on cell invasion and migration of WM239 and MM200 cells by using a Transwell plate (Corning, USA) according to the manufacturer's instruction. Briefly, the upper chambers were plated with around $1×10^5$ cells. Then solidified through 4% paraformaldehyde and dyed with crystal violet. The invaded and migrated cells were recorded and calculated.

Analysis of Cell Apoptosis

Approximately 2×10^5 WM239 and MM200 cells were plated on 6-well dishes. Cell apoptosis was analyzed by using the Annexin V-FITC Apoptosis Detection Kit (CST, USA) according to the manufacturer's instruction. Briefly, the cells were collected and washed by binding buffer (BD Biosciences, USA) and were dyed at 25°C, followed by the flow cytometry analysis.

Cell-Cycle Analysis

Approximately 1×10^5 cells were plated on 6-well dishes and treated as indicated. Floating and adherent cells were fixed in cold ethanol (4°C, 70% in PBS) overnight. RNaseA 1(00 µg/mL) was added to the cells at 37°C for 30 minutes, followed by the PI staining (50 µg/mL, 30 minutes) in the dark and the flow cytometric analysis using a FACSCalibur cytometry (Becton Dickinson, New Jersey, USA). About ten thousand events were calculated for each sample and the distribution of cell cycle was analyzed by Cell Quest software (Becton Dickinson, New Jersey, USA).

Luciferase Reporter Gene Assay

The luciferase reporter gene assays were performed by using the Dual-luciferase Reporter Assay System (Promega, USA). Briefly, the cells were treated with the miR-145 mimic, or control mimic, Cyclin D1, and Cyclin D1 mutant fragment were transfected in the cells by using Lipofectamine 3000 (Invitrogen, USA), followed by the analysis of luciferase activities, in which Renilla was applied as a normalized control.

Quantitative Reverse Transcription-PCR (qRT-PCR)

The total RNAs were extracted by TRIZOL (Invitrogen, USA) from the tumor tissues of the mice. The first-strand cDNA was synthesized using Stand cDNA Synthesis Kit (Thermo, USA) as the manufacturer's instruction. The qRT-PCR was carried out by applying SYBR Real-time PCR I kit (Takara, Japan). The standard control for mRNA was GAPDH. Quantitative determination of the mRNA levels was conducted by SYBR GreenPremix Ex TaqTM II Kit (TaKaRa, Japan). The experiments were independently repeated at least three times. The primer sequences are as follows:

miR-145: forward: 5′-CCGGGAATCGCCAACTCAGCCTTAC −3′

miR-145: reverse: 5′-CGGAATCCGTTGCGACCGTGATACC −3′

Cyclin D1: forward: 5′-AGGAAGTTGTGCCAA TTTTG −3′

Cyclin D1: reverse: 5′-AGCAGATGGCCATGCCTTCT −3′,

U6: forward: 5′-GACCGATTCGTTCTGTGGCAC-3′

U6: reverse: 5′-GATTACCCGTCGGCCATCGATC-3′

GAPDH forward: 5′-AAGAAGGTGGTGAAGC AGGC-3′

GAPDH reverse: 5′-TCCACCACCCAGTTGCTG TA-3′

Western Blot Analysis

Total protein was extracted from the cells or tumor tissues of the mice with RIPA buffer (CST, USA). Protein concentration was measured by using the BCA Protein Quantification Kit (Abbkine, USA). Same concentration of protein was divided by SDS-PAGE (12% polyacrylamide gels), transferred to PVDF membranes (Millipore, USA) in the subsequent step. The membranes were hindered with 5% milk and hatched overnight at 4°C with the primary antibodies for Cyclin D1 (1:1000) (Abcam, USA), p-γH2AX (1:1000) (Abcam, USA), γH2AX (1:1000) (Abcam, USA), and β-actin (1:1000) (Abcam, USA), in which β-actin served as the control. Then, the corresponding second antibodies (1:1000) (Abcam, UK) were used for hatching the membranes 1 hour at room temperature, followed by the visualization by using an Odyssey CLx Infrared Imaging System. The results of Western blot analysis were quantified by ImageJ software.

Analysis of Tumorigenicity in Nude Mice

The effect of the BGM on tumor growth of melanoma in vivo was analyzed in nude mice of Balb/c (male, 4-week-old). To establish in vivo tumor model, the 2×10^6 WM239 cells were subcutaneously injected in the mice. The mice were randomly separated into two groups (n=6). The mice in the BGM group were intraperitoneally treated with BGM (10 mg/kg, 5 days/week). After 7 days of injection, we measured tumor growth every 7 days. We sacrificed the mice after 35 days of injection, and tumors were scaled. Balb/c mice were anesthetized by intraperitoneal injection of 10% chloral hydrate (400 mg/kg). Tumor volume (V) was observed by estimating the length and width with calipers and measured with the method × 0.5. The expression levels of Ki-67 of the tumor tissues were tested by immunohistochemical staining with the Ki67 antibody (CST, USA). Tumor tissues from mice were fixed using neutral buffered

formalin (10%) and embedded in paraffin, which were subjected into the preparation of 4μM-thick sections. The slides were immunohistochemically stained using Ki67 antibody (CST, USA). The protein expression levels of Cyclin D1 (1:1000) (Abcam, USA) were analyzed by Western blot analysis in the tumor tissues of the mice. Animal care and method procedure were authorized by the Third Affiliated Hospital of Guangzhou Medical University Animal Ethics Committee and Welfare Committee. Procedures also followed the guidelines for the care and use of animals provided by the National Institutes of Health Office of Laboratory Animal Welfare.

Statistical Analysis

Data were presented as mean ± SEM, and the statistical analysis was performed by SPSS software (version 18.0). The unpaired Student's *t*-test was applied for comparing two groups, and the one-way ANOVA was applied for comparing among multiple groups. $P < 0.05$ were considered as statistically significant.

Results
BGM Inhibits the Cell Proliferation of Melanoma Cells

To assess the effect of BGM on the cell proliferation of melanoma, the CCK-8 assays and colony formation assays were performed in the WM239 and MM200 cells treated with BGM at the indicated dose. CCK-8 assays showed that the cell viability was significantly repressed by the treatment of BGM in a dose-dependent manner in the WM239 ($P < 0.001$) (Figure 1A) and MM200 cells ($P < 0.001$) (Figure 1B). Similarly, colony formation assays revealed that the colony numbers of WM239 ($P < 0.001$) (Figure 1C) and MM200 cells ($P < 0.001$) (Figure 1D) were remarkably reduced by BGM treatment. Together, these data suggest that BGM is able to inhibit cell proliferation of melanoma.
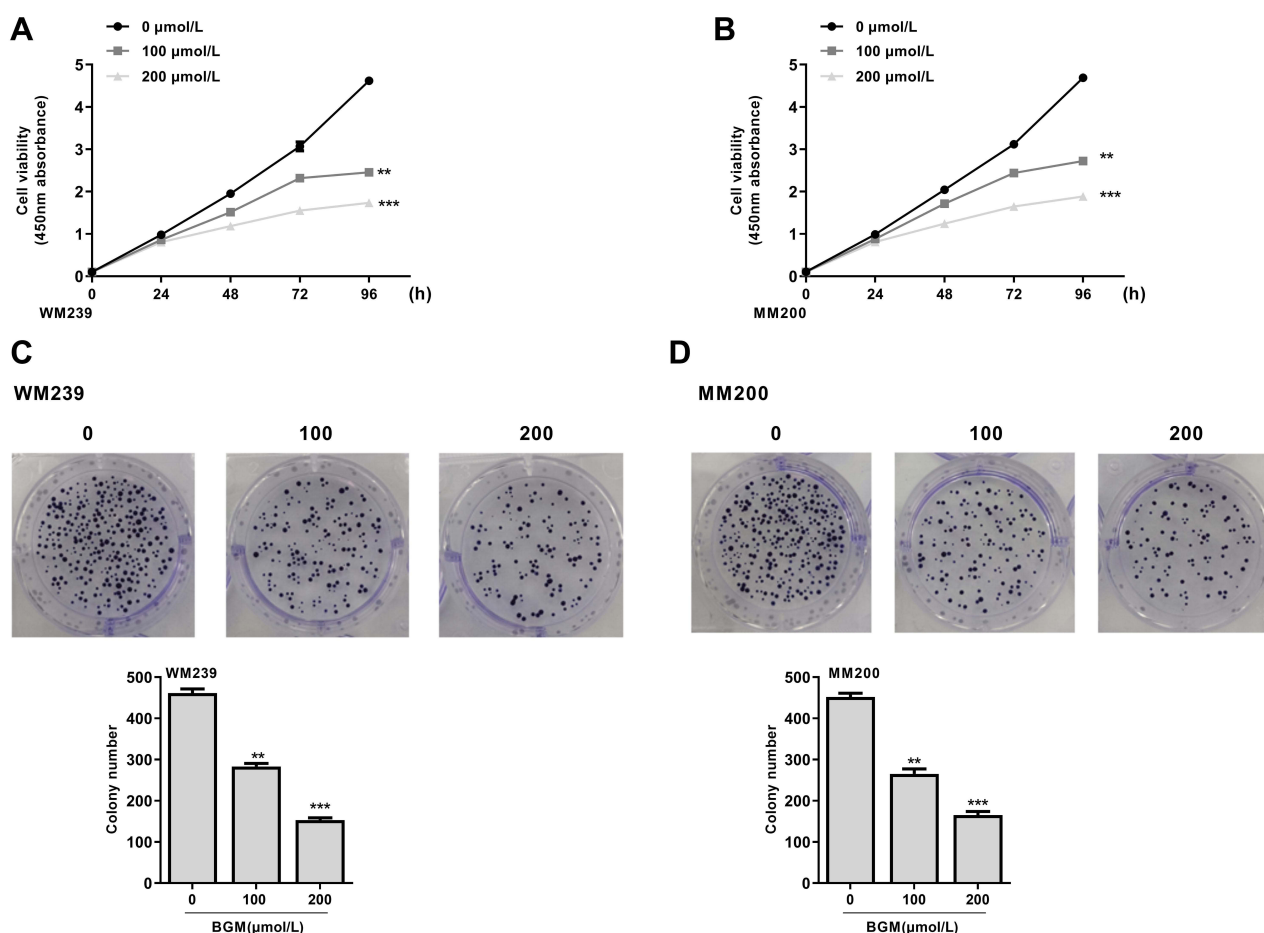

Figure 1 BGM inhibits the cell proliferation of melanoma cells. (**A–D**) The WM239 and MM200 cells were treated with BGM at the indicated dose. (**A** and **B**) The cell viability was measured by CCK-8 assays in the WM239 and MM200 cells, respectively. (**C** and **D**) The cell proliferation was measured by colony formation assays in the WM239 and MM200 cells, respectively. Data are presented as mean ± SEM. Statistic significant differences were indicated: **$P < 0.01$, ***$P < 0.001$.

BGM Suppresses Melanoma Cell Migration and Invasion

We further analyzed the role of BGM in the migration and invasion of the WM239 and MM200 cells. Transwell assays revealed that BGM treatment remarkably reduced the migration in the WM239 and MM200 cells ($P < 0.001$) (Figure 2A). Similarly, the cell invasion was significantly decreased by BGM in the WM239 and MM200 cells ($P < 0.001$) (Figure 2B). Together, these indicate that BGM restrains the migration and invasion of melanoma cells.

BGM Induces the Cell Cycle Arrest and Apoptosis in the Melanoma Cells

Then, we evaluate the effect of BGM on the cell cycle phase distribution by flow cytometry analysis in the WM239 and MM200 cells. The distribution of the cells in the phases of G1, S, and G2/M was calculated using the Multi-cycle software, respectively. Significantly, the G0/G1 phase cells were enhanced while the S phase and G2/M phase cells were reduced by the treatment of BGM in a dose-dependent manner in the cells ($P < 0.01$) (Figure 3A), suggesting that BGM was able to induce

cell cycle arrest at the G0/G1 phase in the melanoma cells. Meanwhile, flow cytometry analysis showed that cell apoptosis was dose-dependently increased by the BGM treatment in the cells ($P < 0.01$) (Figure 3B).

BGM Induces DNA Damage in the Melanoma Cells

Next, we explored the impact of BGM on the DNA damage in the WM239 and MM200 cells. 4, 6-Diamidino-2-phenylindole (DAPI) staining revealed that the DNA condensation was increased by the BGM treatment in a dose-dependent manner in the WM239 and MM200 cells (Table 1) (Figure 4A). Moreover, the phosphorylation and expression levels of γH2AX, as a DNA damage marker, were dose-dependently enhanced by the treatment of BGM in the WM239 and MM200 cells ($P < 0.01$) (Figure 4B).

BGM Up-Regulates the Expression of miR-145

Next, we further explored the underlying mechanism of the effect of BGM on the development of melanoma in the WM239 and MM200 cells. Significantly, we identified that
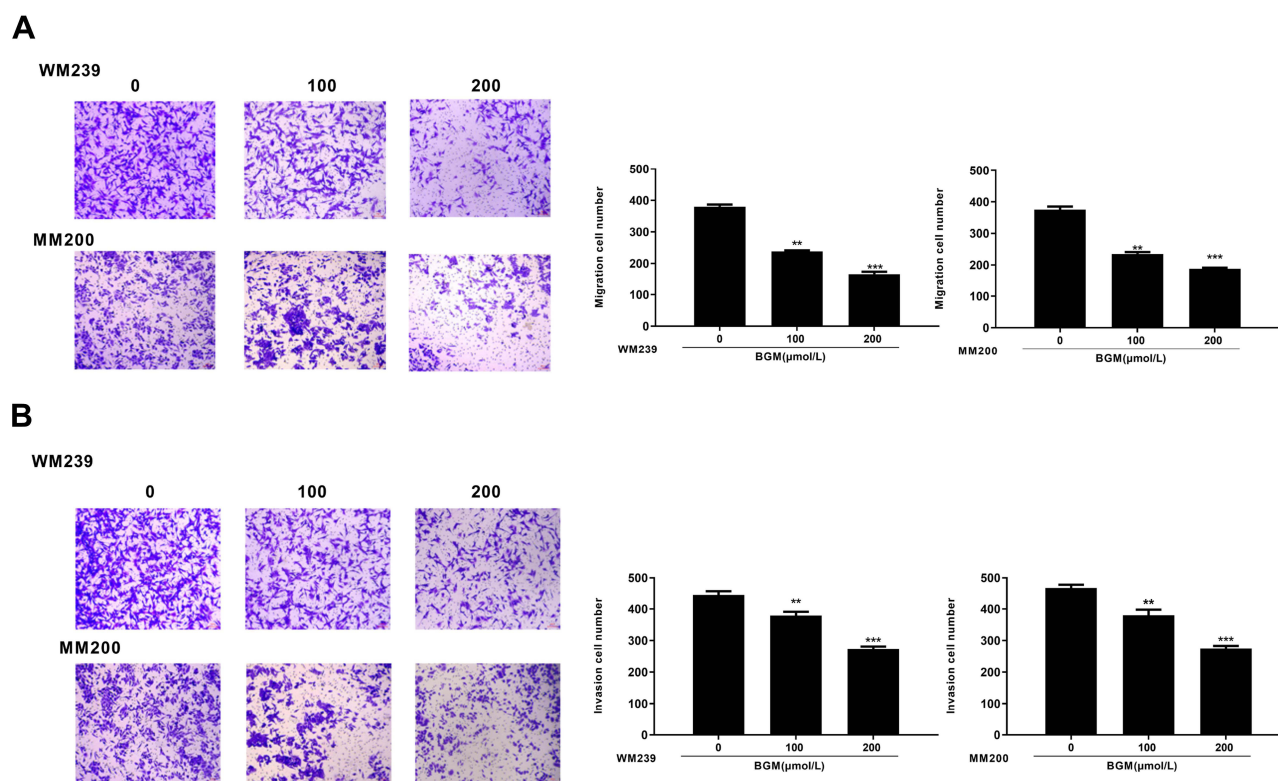

Figure 2 BGM suppresses melanoma cell migration and invasion. (**A** and **B**) The WM239 and MM200 cells were treated with BGM at the indicated dose. (**A**) The cell migration was examined by transwell assays in the cells. (**B**) The cell invasion was examined by transwell assays in the cells. Data are presented as mean ± SEM. Statistic significant differences were indicated: **$P < 0.01$, ***$P < 0.001$.
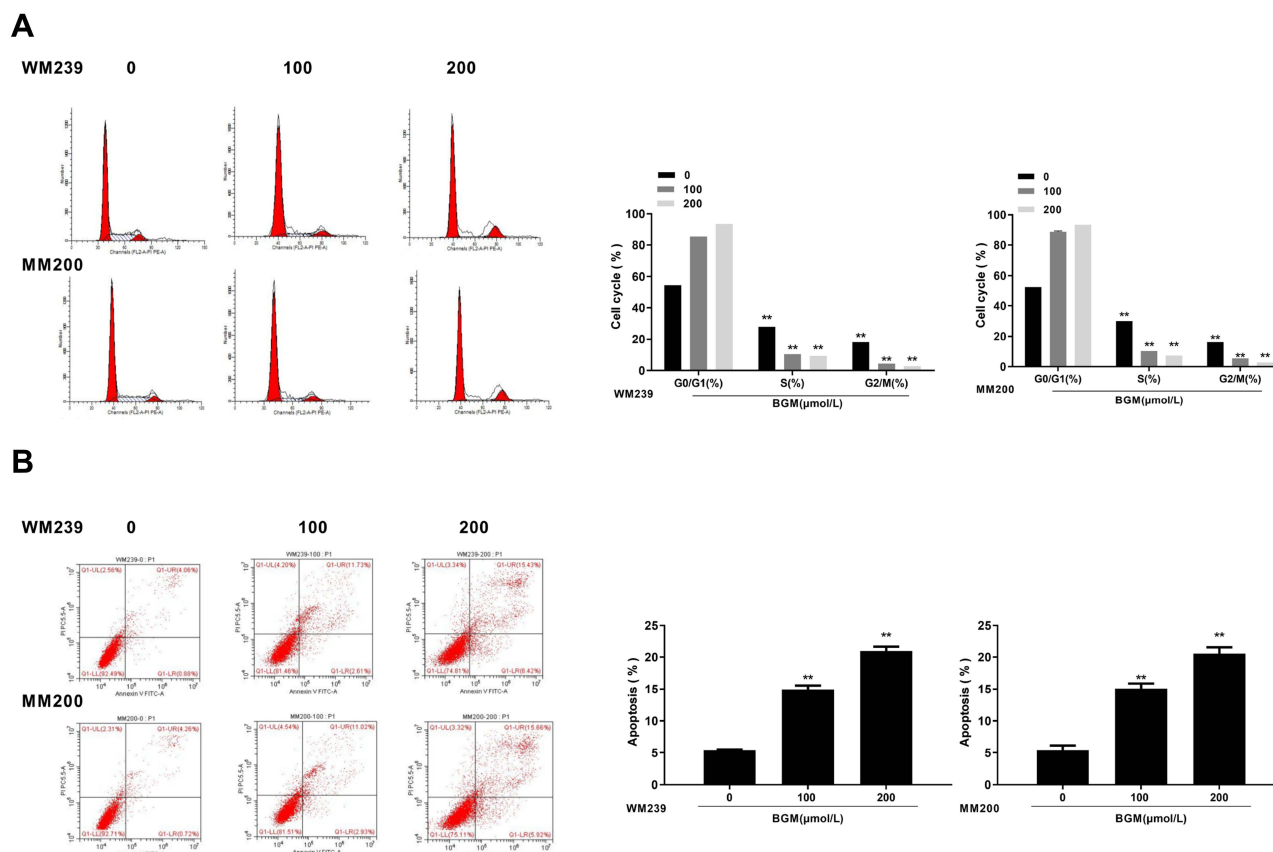
Figure 3 BGM induces the cell cycle arrest and apoptosis in the melanoma cells. (**A** and **B**) The WM239 and MM200 cells were treated with BGM at the indicated dose. (**A**) The cell cycle was analyzed by flow cytometry analysis in the cells. (**B**) The cell apoptosis was measure by flow cytometry analysis in the cells. Data are presented as mean ± SEM. Statistic significant differences were indicated: **$P < 0.01$.

BGM treatment enhanced the expression of miR-145 in the WM239 and MM200 cells ($P < 0.01$) (Figure 5A). The efficiency of miR-145 inhibitor was validated in the cells ($P < 0.01$) (Figure 5B). Moreover, the miR-145 inhibitor reduced but the BGM treatment induced apoptosis of the WM239 and MM200 cells, in which the treatment of the miR-145 inhibitor could block the effect of BGM in the system ($P < 0.01$) (Figure 5C), suggesting that BGM can induce cell apoptosis by the up-regulation of miR-145 in melanoma.

Table 1 Comparison of Tail Length and Comet Rate of Each Group (x ± s, n = 3)

Groups	Comet Length	Comet Rate (%)
BGM 0μmol/L	5.52±0.68	7.02±1.29
BGM 100μmol/L	23.49±3.73**	49.59±1.98**
BGM 200μmol/L	39.95±4.19**	87.75±2.35**

Notes: Data are presented as mean ± SD. **Represents $P < 0.01$ compared with the group of BGM 0μmol/L by unpaired *t*-test.

miR-145 Targets Cyclin D1 in the Melanoma Cells

We then explored the downstream target of miR-145 in the WM239 and MM200 cells. The miR-145-targeted site in Cyclin D1 3′ UTR was identified by a bioinformatic analysis using Targetscan (http://www. targetscan.org/vert_72/) (Figure 5D). The miR-145 mimic treatment inhibited luciferase activities of wild-type Cyclin D1 but failed to affect the Cyclin D1 with the miR-145-binding site mutant in the WM239 and MM200 cells ($P < 0.01$) (Figure 5E). Moreover, the mRNA expression of Cyclin D1 was decreased by miR-145 mimic in the cells ($P < 0.01$) (Figure 5F). Similarly, the protein expression of Cyclin D1 was reduced by the treatment of miR-145 mimic in the cells ($P < 0.01$) (Figure 5G). Together, these data suggest that miR-145 was able to target Cyclin D1 in the melanoma cells.
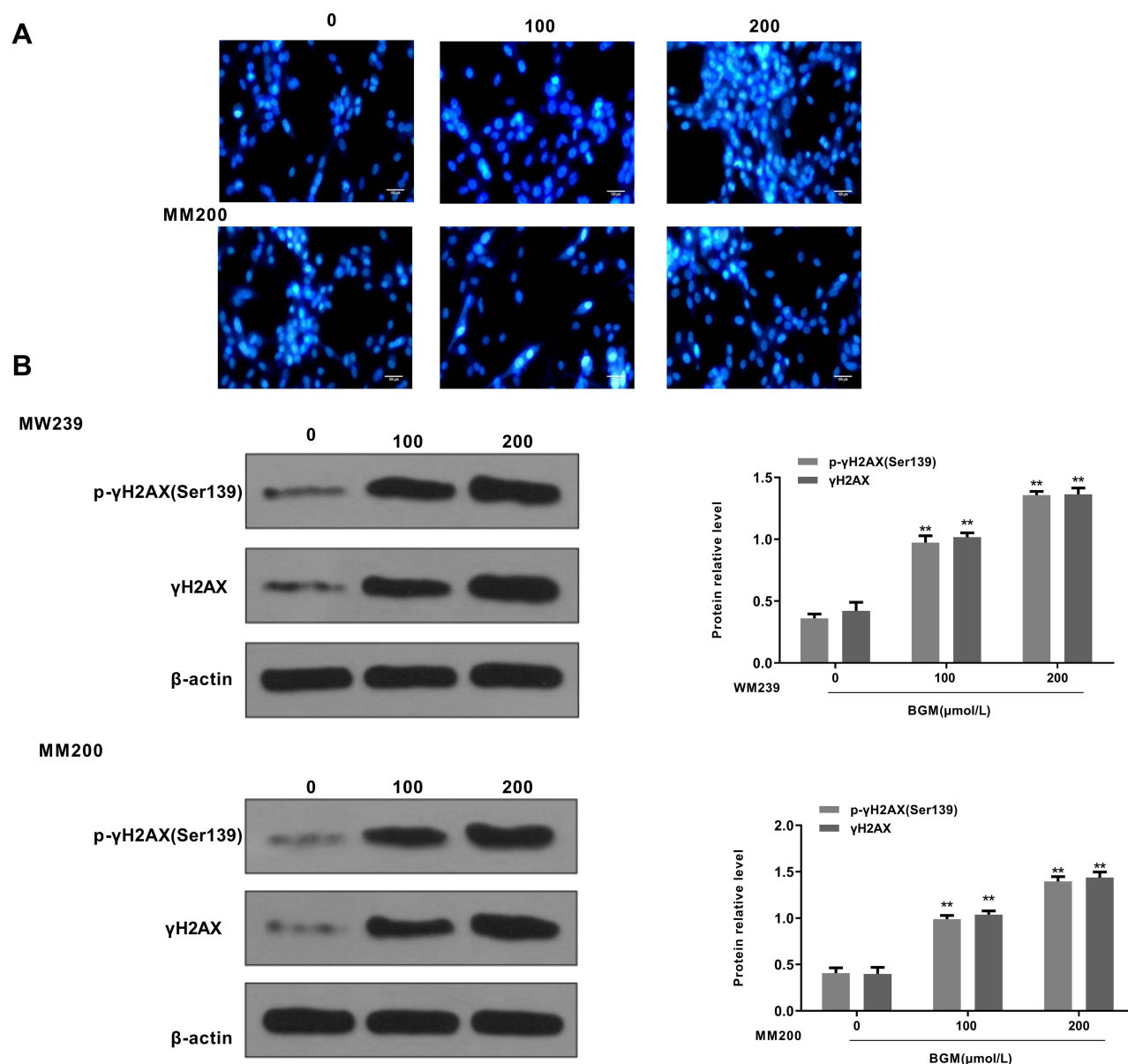
Figure 4 BGM induces DNA damage in the melanoma cells. (**A** and **B**) The WM239 and MM200 cells were treated with BGM at the indicated dose. (**A**) The DNA condensation was analyzed by the 4, 6-Diamidino-2-phenylindole (DAPI) staining in the cells. (**B**) The γH2AX phosphorylation (Ser139), expression of γH2AX and β-actin were measured by Western blot analysis in the cells. The results of Western blot analysis were quantified by ImageJ software. Data are presented as mean ± SEM. Statistic significant differences were indicated: **$P < 0.01$.

BGM Inhibits the Progression of Melanoma by Targeting miR-145/Cyclin D1 Axis in vitro

We then further investigated whether BGM induced the inhibitory effect on melanoma progression by modulating miR-145/Cyclin D1 axis in vitro. The mRNA expression of Cyclin D1 was down-regulated by the BGM treatment in the WM239 and MM200 cells ($P < 0.01$) (Figure 6A). Similarly, BGM could reduce the protein expression of Cyclin D1 in the

cells ($P < 0.01$) (Figure 6B). Meanwhile, the treatment of miR-145 inhibitor was able to rescue the expression of Cyclin D1 inhibited by BGM in the cells ($P < 0.01$) (Figure 6C). The efficiency of Cyclin D1 overexpression was validated in the cells ($P < 0.01$) (Figure 6D). Moreover, BGM treatment was able to decrease the cell viability of the WM239 and MM200 cells, in which the overexpression of Cyclin D1 rescued this phenotype ($P < 0.01$) (Figure 6E). Besides, the Cyclin D1 overexpression
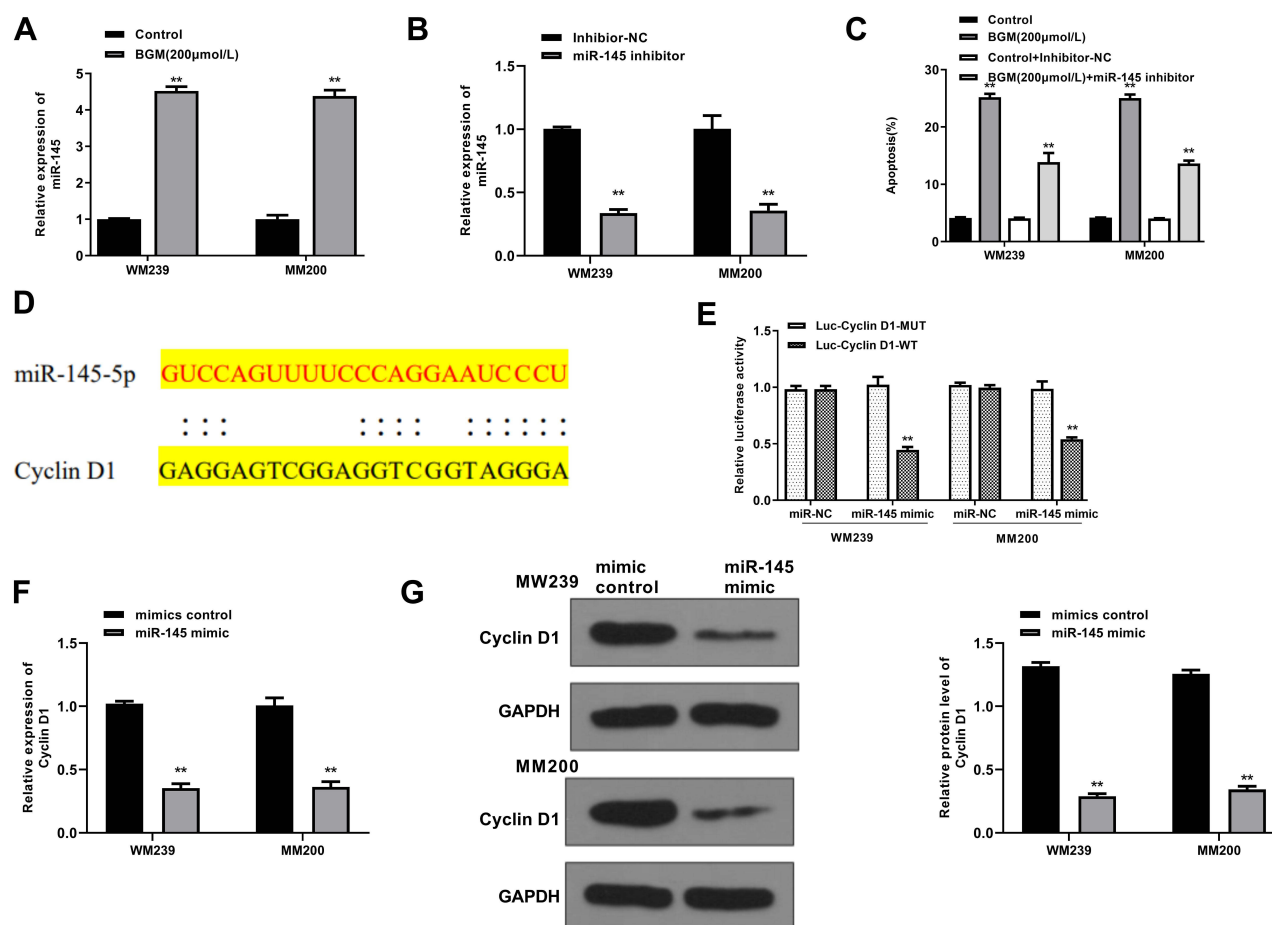
Figure 5 BGM targets Cyclin D1 by up-regulating the expression of miR-145. (**A**) The WM239 and MM200 cells were treated with BGM at the indicated dose. The expression of miR-145 was measured by qPCR assays in the cells. (**B**) The WM239 and MM200 cells were treated with miR-145 inhibitor. The expression of miR-145 was measured by qPCR assays in the cells. (**C**) The WM239 and MM200 cells were treated with BGM at indicated dose, control inhibitor, or co-treated with BGM and miR-145 inhibitor. The cell apoptosis was measure by flow cytometry analysis in the cells. (**D**) The interaction of miR-145 and Cyclin D1 3′ UTR was identified by bioinformatic analysis using Targetscan (http://www.targetscan.org/vert_72/). (**E–G**) The WM239 and MM200 cells were treated with control mimic or miR-145 mimic. (**E**) The luciferase activities of wild type Cyclin D1 (Cyclin D1 WT) and Cyclin D1 with the miR-145-binding site mutant (Cyclin D1 MUT) were determined by luciferase reporter gene assays in the cells. (**F**) The mRNA expression of Cyclin D1 was assessed by qPCR assays in the cells. (**G**) The protein expression of Cyclin D1 and β-actin was tested by Western blot analysis in the cells. The results of Western blot analysis were quantified by ImageJ software. Data are presented as mean ± SEM. Statistic significant differences were indicated: **P < 0.01.

could attenuate the apoptosis induced by BGM treatment in the cells (P < 0.01) (Figure 6F). Together, these suggest that BGM inhibits the progression of melanoma by targeting miR-145/Cyclin D1 axis in vitro.

BGM Inhibits Tumor Growth of Melanoma in vivo

Then, we further investigated the effect of BGM on melanoma development in vivo. For this purpose, we performed the tumorigenicity analysis in the nude mice injected with WM239 cells, which were treated with BGM or corresponding control. The BGM treatment significantly reduced tumor size (Figure 7A), tumor weight (P < 0.01) (Figure 7B), tumor volume (P < 0.01) (Figure 7C), and the expression of Ki-67 (Figure 7D) and Cyclin D1 (Figure 7E) in the tumor tissues of the mice, suggesting that BGM inhibits tumor growth of melanoma in vivo.

Discussion

Melanoma serves as prevailing skin cancer, in which the patients hold low prognosis and poor survival rates.[1] Although the developments in chemotherapy, radiotherapy, and surgery, metastasis and drug resistance are still the principal causes of melanoma-related mortality, and it is urgent to find more safe and practical treatment candidates for the
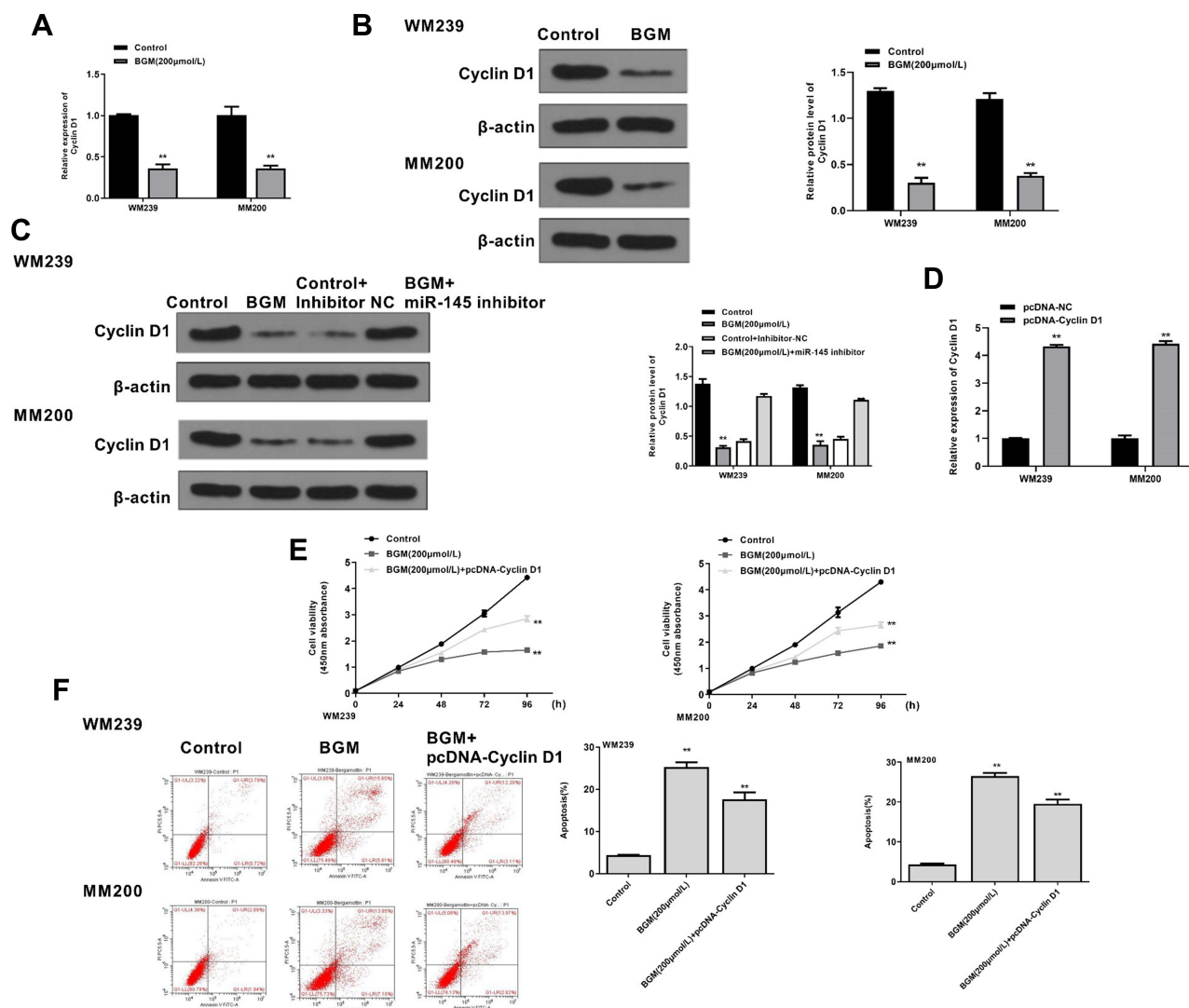
Figure 6 BGM inhibits the progression of melanoma by targeting miR-145/Cyclin D1 axis in vitro. (**A** and **B**) The WM239 and MM200 cells were treated with BGM at indicated dose. (**A**) The mRNA expression of Cyclin D1 was assessed by qPCR assays in the cells. (**B**) The protein expression of Cyclin D1 and was tested by Western blot analysis in the cells. The results of Western blot analysis were quantified by ImageJ software. (**C**) The WM239 and MM200 cells were treated with BGM at the indicated dose, control inhibitor, or co-treated with BGM and miR-145 inhibitor. The protein expression of Cyclin D1 and β-actin was measured by Western blot analysis in the cells. (**D**) The WM239 and MM200 cells were transfected with pcDNA control vector or pcDNA-Cyclin D1 overexpression vector. The expression of Cyclin D1 was analyzed by qPCR assays in the cells. (**E** and **F**) The WM239 and MM200 cells were treated with BGM at the indicated dose or co-treated with BGM and pcDNA-Cyclin D1 overexpression vector. (**E**) The cell viability was measured by CCK-8 assays in the cells. (**F**) The cell apoptosis was measure by flow cytometry analysis in the cells. Data are presented as mean ± SEM. Statistic significant differences were indicated: $**P < 0.01$.

effective therapy of melanoma.[4] Bergamottin (BGM), as a natural furanocoumarin obtained from grapefruits, displays the potential anti-cancer activity in several tumor models.[14] It has been reported that BGM, combined with simvastatin, exerts anti-cancer effects on human chronic myelogenous leukemia by regulating the NF-κB signaling.[29] The anti-tumor influences of BGM on abolishing the activity of phorbol-12-myristate-13-acetate-stimulated MMP-9 and invasion of human fibrosarcoma cells are identified.[30] Bergamottin is able to suppress human glioma cells' invasiveness through the inactivation of the Rac1 pathway.[31] Bergamottin presents

an anti-tumor function in lung adenocarcinoma by the stimulation of mitochondrial membrane potential loss, cell cycle arrest, and apoptosis, and the decrease of cell invasion and migration in vitro and in vivo.[32] Bergamottin is able to inhibit lung cancer cells' metastasis by the attenuation of epithelial-to-mesenchymal transition and several oncogenes signaling cascades.[33] The anti-proliferation function of bergamottin in the promyelocytic leukemia HL-60 cells and the cytotoxic impact of bergamottin against the gastric cancer NCI-N87 cells have been previously reported as well.[34,35] In this study, we firstly identified that BGM inhibited cell proliferation,
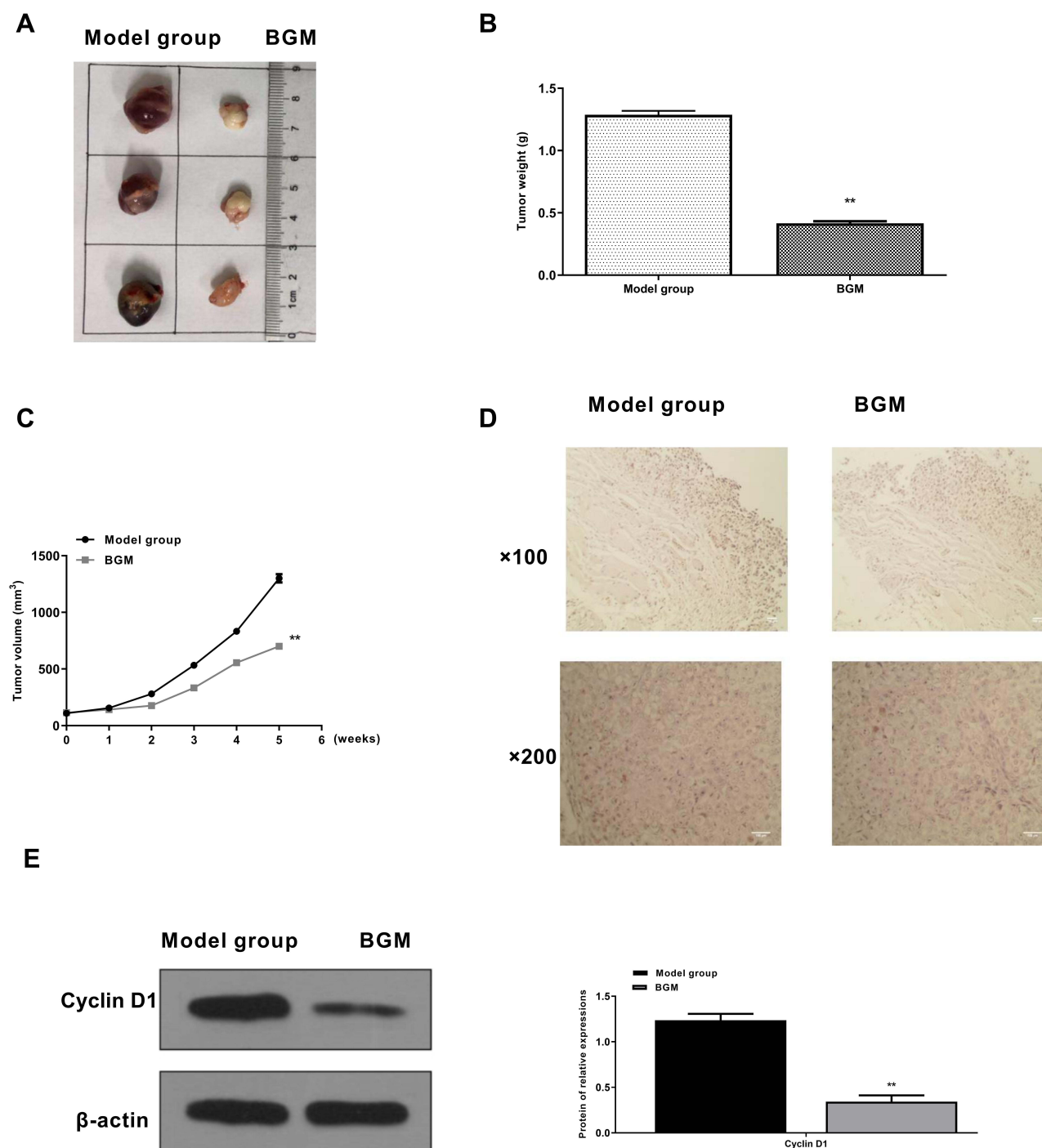
Figure 7 BGM inhibits tumor growth of melanoma in vivo. (**A–D**) The effect of BGM on tumor growth of melanoma in vivo was analyzed by nude mice tumorigenicity assay. The WM239 cells were injected into the nude mice (n = 6). The mice in the BGM group were intraperitoneally treated with BGM (10 mg/kg) (**A**) Representative images of dissected tumors from nude mice were presented. (**B**) The average tumor weight was calculated and shown. (**C**) The average tumor volume was calculated and shown. (**D**) The expression levels of Ki-67 of the tumor tissues were measured by immunohistochemical staining. (**E**) The expression of Cyclin D1 was measured by Western blot analysis in the tumor tissues of the mice. The results of Western blot analysis were quantified by ImageJ software. Data are presented as mean ± SEM. Statistic significant differences were indicated: ** $P < 0.01$.

migration, invasion, and induced cell cycle arrest, cell apoptosis, and DNA damage of melanoma cells. BGM reduced the tumor growth of melanoma in vivo. These data present a novel inhibitory function of the BGM in melanoma, providing valuable evidence of the application of BGM in cancer development. More details of BGM-mediated DNA damage are needed to explore in the future by other experiments.

MiRNAs serve as the essential factor for posttranscriptional gene regulation through targeting mRNAs and contribute to the development of cancers, including melanoma, by modulating crucial pathways.[16,21] It has been reported that miR-424 serves as the potential biomarker for the diagnosis and prognosis in melanoma.[36] MiR-410-3p stimulated by vemurafenib by ER stress contributes to the BRAF inhibitor resistance in melanoma.[21] MiR-33a-5p represses the metastasis and growth of melanoma cells by modulating the expression of SNAI2.[37] MR-489-3p/SIX1 signaling modulates the glycolytic potential and cell proliferation in melanoma.[38] Moreover, the role of miRNA-145 in the modulation of melanoma has been identified. It has been revealed that miRNA-145 is able to suppress the angiogenesis and growth of uveal melanoma by modulating vascular endothelial growth factor and viral oncogene homolog of neuroblastoma RAS.[24] Circular RNA circ_0017247 increases the invasion and migration of melanoma by targeting miR-145.[39] MiRNA-145 represses the tumor metastasis and occurrence by the modulation of NF-κB signaling through regulating TLR4 in the malignant melanoma.[40] Impacts of miR-145-5p by NRAS on invasion, migration, apoptosis, and cell proliferation of melanoma by repressing PI3K/AKT and MAPK signaling.[41] MiRNA-145 may perform an essential function in the modulation of cell growth through potentially controlling insulin receptor substrate-1 in uveal melanoma.[42] The overexpression of miR-145 represses the invasion and migration of metastatic melanoma cells.[43] Our data demonstrated that BGM could enhance the expression of miR-145 in melanoma cells and BGM was able to induce cell apoptosis by the up-regulation of miR-145 in melanoma. It presents the valuable information that BGM exerts its an-tumor function by modulating the expression of miR-145.

As the critical contributor to cancer progression, Cyclin D1 plays crucial roles in the development of melanoma. It has been reported that expression of Cyclin D1 is elevated in the melanoma patients.[44] MiRNA-365 increases apoptosis and represses growth through modulating BCL2 and Cyclin D1 in melanoma cells.[45] RAF inhibitor LY3009120 stimulates BRAF or RAS mutant tumor to inhibition of CDK4/6 through abemaciclib by exceeding repression of phospho-RB and destruction of cyclin D1.[46] Adhesion regulator of the levels of p27Kip1 and cyclin D1 is deregulated by BRAF/MEK/ERK signaling in melanoma cells.[47] Enhanced expression of cyclin D1 is able to negotiate

the resistance of BRAF inhibitor in BRAF-mutated melanomas.[48] Cyclin D1 controls the degradation of p27Kip1 induced by Cks1/S phase kinase-associated protein 2 in human melanoma cells.[49] In the present study, we revealed that Cyclin D1 was targeted by miR-145 and involved in the mechanism of BGM/miR-145-induced inhibitory effect on the progression of melanoma. It reveals an unreported correlation of Cyclin D1 with BGM and miR-145 in the development of melanoma, validating the crucial role of Cyclin D1 in melanoma. Moreover, there are some limitations in this study, which are needed to explore further in future investigations. For example, the mice numbers of in vivo tumorigenicity analysis of this study are limited. Meanwhile, the detained investigation and exploration of the useful concentration of BGM anti-tumor function are needed to study. Moreover, the clinical application of BGM in the treatment of melanoma is needed to confirm in the future.

Conclusions

We discovered that BGM induced DNA damage and attenuated melanoma progression by modulating miR-145/Cyclin D1 axis. Our finding provides new insights into the mechanism by which BGM modulates the development of melanoma. BGM may be applied as a potential anti-tumor candidate for melanoma in clinical treatment strategy.

Abbreviations

BGM, Bergamottin; miRNAs, microRNAs.

Disclosure

The authors declare no competing interests including financial interests.

References

1. McNally RJQ, Basta NO, Errington S, James PW, Norman PD, Craft AW. Socioeconomic patterning in the incidence and survival of children and young people diagnosed with malignant melanoma in northern England. *J Invest Dermatol*. 2014;134(11):2703–2708. doi:10.1038/jid.2014.246

2. Miller AJ, Mihm MC Jr. Melanoma. *N Engl J Med*. 2006;355 (1):51–65. doi:10.1056/NEJMra052166

3. Bedogni B, Paus R. Hair(y) matters in melanoma biology. *Trends Mol Med*. 2020;26(5):441–449. doi:10.1016/j.molmed.2020.02.005

4. Rishi A, Yu HM. Current treatment of melanoma brain metastasis. *Curr Treat Options Oncol*. 2020;21(6):45. doi:10.1007/s11864-020-00733-z

5. Malvi P, Chaube B, Singh SV, et al. Elevated circulatory levels of leptin and resistin impair therapeutic efficacy of dacarbazine in melanoma under obese state. *Cancer Metab*. 2018;6(1):2. doi:10.1186/s40170-018-0176-5

6. Mohammad N, Malvi P, Meena AS, et al. Cholesterol depletion by methyl-beta-cyclodextrin augments tamoxifen induced cell death by enhancing its uptake in melanoma. *Mol Cancer*. 2014;13(1):204. doi:10.1186/1476-4598-13-204

7. Malvi P, Chaube B, Singh SV, et al. Weight control interventions improve therapeutic efficacy of dacarbazine in melanoma by reversing obesity-induced drug resistance. *Cancer Metab*. 2016;4(1):21. doi:10.1186/s40170-016-0162-8

8. Abildgaard C, Guldberg P. Molecular drivers of cellular metabolic reprogramming in melanoma. *Trends Mol Med*. 2015;21(3):164–171. doi:10.1016/j.molmed.2014.12.007

9. Xu-Monette ZY, Zhang M, Li J, Young KH. PD-1/PD-L1 blockade: have we found the key to unleash the antitumor immune response? *Front Immunol*. 2017;8:1597.

10. Flaherty KT, Infante JR, Daud A, et al. Combined BRAF and MEK inhibition in melanoma with BRAF V600 mutations. *N Engl J Med*. 2012;367(18):1694–1703. doi:10.1056/NEJMoa1210093

11. Shanmugam MK, Lee JH, Chai EZ, et al. Cancer prevention and therapy through the modulation of transcription factors by bioactive natural compounds. *Semin Cancer Biol*. 2016;40–41:35–47. doi:10.1016/j.semcancer.2016.03.005

12. Bishayee A, Sethi G. Bioactive natural products in cancer prevention and therapy: progress and promise. *Semin Cancer Biol*. 2016;40–41:1–3. doi:10.1016/j.semcancer.2016.08.006

13. Hung WL, Suh JH, Wang Y. Chemistry and health effects of furanocoumarins in grapefruit. *J Food Drug Anal*. 2017;25(1):71–83. doi:10.1016/j.jfda.2016.11.008

14. Ko JH, Arfuso F, Sethi G, Ahn KS. Pharmacological utilization of bergamottin, derived from grapefruits, in cancer prevention and therapy. *Int J Mol Sci*. 2018;19(12):4048. doi:10.3390/ijms19124048

15. Kim SM, Lee JH, Sethi G, et al. Bergamottin, a natural furanocoumarin obtained from grapefruit juice induces chemosensitization and apoptosis through the inhibition of STAT3 signaling pathway in tumor cells. *Cancer Lett*. 2014;354(1):153–163. doi:10.1016/j.canlet.2014.08.002

16. Lu TX, Rothenberg ME. MicroRNA. *J Allergy Clin Immunol*. 2018;141(4):1202–1207. doi:10.1016/j.jaci.2017.08.034

17. Ghafouri-Fard S, Vafaee R, Shoorei H, Taheri M. MicroRNAs in gastric cancer: biomarkers and therapeutic targets. *Gene*. 2020;757:144937. doi:10.1016/j.gene.2020.144937

18. Otoukesh B, Abbasi M, Gorgani HO, et al. MicroRNAs signatures, bioinformatics analysis of miRNAs, miRNA mimics and antagonists, and miRNA therapeutics in osteosarcoma. *Cancer Cell Int*. 2020;20:254.

19. Aali M, Mesgarzadeh AH, Najjary S, Abdolahi HM, Kojabad AB, Baradaran B. Evaluating the role of microRNAs alterations in oral squamous cell carcinoma. *Gene*. 2020;757:144936. doi:10.1016/j.gene.2020.144936

20. Ross CL, Kaushik S, Valdes-Rodriguez R, Anvekar R. MicroRNAs in cutaneous melanoma: role as diagnostic and prognostic biomarkers. *J Cell Physiol*. 2018;233(7):5133–5141. doi:10.1002/jcp.26395

21. Grzywa TM, Klicka K, Paskal W, et al. miR-410-3p is induced by vemurafenib via ER stress and contributes to resistance to BRAF inhibitor in melanoma. *PLoS One*. 2020;15(6):e0234707. doi:10.1371/journal.pone.0234707

22. Motti ML, Minopoli M, Di Carluccio G, Ascierto PA, Carriero MV. MicroRNAs as key players in melanoma cell resistance to MAPK and immune checkpoint inhibitors. *Int J Mol Sci*. 2020;21(12):4544. doi:10.3390/ijms21124544

23. Li YF, Dong L, Li Y, Wei WB. A review of MicroRNA in uveal melanoma. *Onco Targets Ther*. 2020;13:6351–6359. doi:10.2147/OTT.S253946

24. Yang JY, Li Y, Wang Q, Zhou WJ, Yan YN, Wei WB. MicroRNA-145 suppresses uveal melanoma angiogenesis and growth by targeting neuroblastoma RAS viral oncogene homolog and vascular endothelial growth factor. *Chin Med J (Engl)*. 2020.

25. Stark MS, Gray ES, Isaacs T, et al. A panel of circulating MicroRNAs detects uveal melanoma with high precision. *Transl Vis Sci Technol*. 2019;8(6):12. doi:10.1167/tvst.8.6.12

26. Li X, Ren Z, Yao Y, Bao J, Yu Q. The circular RNA circEIF3M promotes breast cancer progression by promoting cyclin D1 expression. *Aging (Albany NY)*. 2020;12.

27. Li J, Liao P, Wang K, et al. Calcium sensing receptor inhibits growth of human lung adenocarcinoma possibly via the GSK3beta/Cyclin D1 pathway. *Front Cell Dev Biol*. 2020;8:446. doi:10.3389/fcell.2020.00446

28. Zhang H, Pu J, Qi T, et al. MicroRNA-145 inhibits the growth, invasion, metastasis and angiogenesis of neuroblastoma cells through targeting hypoxia-inducible factor 2 alpha. *Oncogene*. 2014;33(3):387–397. doi:10.1038/onc.2012.574

29. Kim SM, Lee EJ, Lee JH, et al. Simvastatin in combination with bergamottin potentiates TNF-induced apoptosis through modulation of NF-kappaB signalling pathway in human chronic myelogenous leukaemia. *Pharm Biol*. 2016;54(10):2050–2060. doi:10.3109/13880209.2016.1141221

30. Hwang YP, Yun HJ, Choi JH, Kang KW, Jeong HG. Suppression of phorbol-12-myristate-13-acetate-induced tumor cell invasion by bergamottin via the inhibition of protein kinase Cdelta/p38 mitogen-activated protein kinase and JNK/nuclear factor-kappaB-dependent matrix metalloproteinase-9 expression. *Mol Nutr Food Res*. 2010;54(7):977–990. doi:10.1002/mnfr.200900283

31. Luo W, Song Z, Sun H, Liang J, Zhao S. Bergamottin, a natural furanocoumarin abundantly present in grapefruit juice, suppresses the invasiveness of human glioma cells via inactivation of Rac1 signaling. *Oncol Lett*. 2018;15(3):3259–3266. doi:10.3892/ol.2017.7641

32. Wu HJ, Wu HB, Zhao YQ, Chen LJ, Zou HZ. Bergamottin isolated from Citrus bergamia exerts in vitro and in vivo antitumor activity in lung adenocarcinoma through the induction of apoptosis, cell cycle arrest, mitochondrial membrane potential loss and inhibition of cell migration and invasion. *Oncol Rep*. 2016;36(1):324–332. doi:10.3892/or.2016.4833

33. Ko JH, Nam D, Um JY, Jung SH, Sethi G, Ahn KS. Bergamottin suppresses metastasis of lung cancer cells through abrogation of diverse oncogenic signaling cascades and epithelial-to-mesenchymal transition. *Molecules*. 2018;23(7):1601. doi:10.3390/molecules23071601

34. Liu Y, Ren C, Cao Y, et al. Characterization and purification of bergamottin from Citrus grandis (L.) osbeck cv. yongjiazaoxiangyou and its antiproliferative activity and effect on glucose consumption in HepG2 cells. *Molecules*. 2017;22(7).

35. Sekiguchi H, Washida K, Murakami A. Suppressive effects of selected food phytochemicals on CD74 expression in NCI-N87 gastric carcinoma cells. *J Clin Biochem Nutr*. 2008;43(2):109–117. doi:10.3164/jcbn.2008054

36. Xu SJ, Xu WJ, Zeng Z, Zhang M, Zhang DY. MiR-424 functions as potential diagnostic and prognostic biomarker in melanoma. *Clin Lab*. 2020;66(7). doi:10.7754/Clin.Lab.2019.190917

37. Zhang ZR, Yang N. MiR-33a-5p inhibits the growth and metastasis of melanoma cells by targeting SNAI2. *Neoplasma*. 2020;67(04):813–824. doi:10.4149/neo_2020_190823N811

38. Yang X, Zhu X, Yan Z, et al. miR-489-3p/SIX1 axis regulates melanoma proliferation and glycolytic potential. *Mol Ther Oncolytics*. 2020;16:30–40. doi:10.1016/j.omto.2019.11.001

39. Chen Z, Kang K, Chen S, et al. Circular RNA circ_0017247 promotes melanoma migration and invasion via targeting miR-145. *Eur Rev Med Pharmacol Sci*. 2020;24(4):1932–1938. doi:10.26355/eurrev_202002_20371

40. Jin C, Wang A, Liu L, Wang G, Li G, Han Z. miR-145-5p inhibits tumor occurrence and metastasis through the NF-kappaB signaling pathway by targeting TLR4 in malignant melanoma. *J Cell Biochem*. 2019;120(7):11115–11126. doi:10.1002/jcb.28388

41. Liu S, Gao G, Yan D, et al. Effects of miR-145-5p through NRAS on the cell proliferation, apoptosis, migration, and invasion in melanoma by inhibiting MAPK and PI3K/AKT pathways. *Cancer Med*. 2017;6 (4):819–833. doi:10.1002/cam4.1030

42. Li Y, Huang Q, Shi X, et al. MicroRNA 145 may play an important role in uveal melanoma cell growth by potentially targeting insulin receptor substrate-1. *Chin Med J (Engl)*. 2014;127(8):1410–1416.

43. Dynoodt P, Speeckaert R, De Wever O, et al. miR-145 overexpression suppresses the migration and invasion of metastatic melanoma cells. *Int J Oncol*. 2013;42(4):1443–1451. doi:10.3892/ijo.2013.1823

44. Kaufmann C, Kempf W, Mangana J, et al. The role of cyclin D1 and Ki-67 in the development and prognostication of thin melanoma. *Histopathology*. 2020;77(3):460–470. doi:10.1111/his.14139

45. Zhu Y, Wen X, Zhao P. MicroRNA-365 inhibits cell growth and promotes apoptosis in melanoma by targeting BCL2 and cyclin D1 (CCND1). *Med Sci Monit*. 2018;24:3679–3692. doi:10.12659/MSM.909633

46. Chen SH, Gong X, Zhang Y, et al. RAF inhibitor LY3009120 sensitizes RAS or BRAF mutant cancer to CDK4/6 inhibition by abemaciclib via superior inhibition of phospho-RB and suppression of cyclin D1. *Oncogene*. 2018;37(6):821–832. doi:10.1038/onc.2017.384

47. Bhatt KV, Spofford LS, Aram G, McMullen M, Pumiglia K, Aplin AE. Adhesion control of cyclin D1 and p27Kip1 levels is deregulated in melanoma cells through BRAF-MEK-ERK signaling. *Oncogene*. 2005;24(21):3459–3471. doi:10.1038/sj.onc.1208544

48. Smalley KS, Lioni M, Dalla Palma M, et al. Increased cyclin D1 expression can mediate BRAF inhibitor resistance in BRAF V600E-mutated melanomas. *Mol Cancer Ther*. 2008;7 (9):2876–2883. doi:10.1158/1535-7163.MCT-08-0431

49. Bhatt KV, Hu R, Spofford LS, Aplin AE. Mutant B-RAF signaling and cyclin D1 regulate Cks1/S-phase kinase-associated protein 2-mediated degradation of p27Kip1 in human melanoma cells. *Oncogene*. 2007;26(7):1056–1066. doi:10.1038/sj.onc.1209861